JOURNAL OF BACTERIOLOGY, July 1992, p. 4811–4819
0021-9193/92/144811-09$02.00/0

Vol. 174, No. 14

Elasticity of the Sacculus of *Escherichia coli*

ARTHUR L. KOCH[1]* AND STEVEN WOESTE[2]

Department of Biology, Indiana University, Bloomington, Indiana 47405,[1] and Department of Natural Sciences, Indiana University, Kokomo, Indiana 46904[2]

Received 4 February 1992/Accepted 17 April 1992

Preparations of purified peptidoglycan of *Escherichia coli* (i.e., sacculi) were studied by low-angle laser light scattering. Control experiments and theoretical calculations based on the Rayleigh-Gans theory showed that the mean sacculus surface area could be accurately inferred from measurements with our apparatus by using computer routines developed previously. Large changes in the mean saccular surface area resulted from alterations in the stress caused by varying the net charge on the sacculi. The net charge was affected by altering the suspending medium pH, causing carboxyl and amino groups in the peptidoglycan to gain or lose protons, or by acetylation or succinylation of the amino groups. A preponderance of either plus or minus charges caused an expansion of the mean sacculus surface area. The largest increase in area probably represents the elastic limit of the peptidoglycan and was 300% above the area of isoionic sacculi. This degree of expansion is consistent with possible conformations of the intact peptidoglycan structure without necessitating rupture of the wall fabric. Our findings concerning saccular elasticity provide support for the surface stress theory. It provides a mechanism so that bacteria can grow and divide while maintaining turgor pressure, without the necessity of having and using proteins to do the mechanical work.

It is now well established that the peptidoglycan sacculus is the stress-resistant, shape-determining structure covering the procaryotic cell (4, 23, 27–29, 34, 37, 42, 45, 46, 49, 63, 72). Its covalent structure makes the sacculus the largest macromolecule in nature and imparts strength to the bacterial wall. Additionally, the ability of the sacculus to stretch is of fundamental importance, both for giving flexibility to the organism and providing a mechanism for its enlargement during growth. The elasticity, as measured by Young's modulus, is the inverse of the ratio that a body is stretched (strain) by a given force (stress) (71). At high-enough stress, a body's elastic limit is reached, and it cannot be stretched further without the rupture of integral covalent bonds. Elastic enlargement of a single cell's wall fabric, composed of cross-linked peptidoglycan, depends on conformational changes that involve only rotations and easily made rearrangements of hydrogen bonds. Enlargement exceeding the elasticity must involve the rupture (hydrolysis in an aqueous environment) of covalent bonds (37, 40).

Sacculi are too small to have either their elasticity or their rupture limit (extensibility) measured by engineering materials testing methods (71). Although the sacculus cannot be affixed at two ends and mechanically stretched, the relationship between the sacculus net charge and surface area can be determined. We studied sacculi of *Escherichia coli* from cultures in balanced exponential growth. They were prepared free of almost all nonpeptidoglycan materials. The mean surface area of the sacculi under different conditions was measured by a low-angle laser-light-scattering method. The charge on the sacculi was altered with either acid or base or by either succinylating or acetylating the amino groups of the peptidoglycan. Additionally, the effect of saccular charges was reduced by raising the ionic strength of the medium. The effect of secondary structure was reduced by breaking internal hydrogen bonds with urea.

The sacculus of *E. coli* has a typical gram-negative peptidoglycan composition of polysaccharides and peptides (14, 18, 22, 63, 68). The glycan chains are alternating molecules of *N*-acetyl muramic acid and *N*-acetyl-glucosamine. A small fraction of these amino sugars are unacetylated and therefore can accept protons. At least 60 different kinds of fragments have been identified with high-pressure liquid chromatography of muramidase-treated sacculi (12, 13, 21, 22, 64). Earlier biochemical work (63, 68) showed that each disaccharide of *N*-acetyl muramic acid is β(1-4) linked to *N*-acetyl-glucosamine. A pentapeptide consisting of L-alanyl-D-γ-glutamyl-*meso*-diaminopimelic acid–D-alanyl-D-alanine is covalently attached to the lactyl group of the muramic acid as secreted through the cytoplasmic membrane. However, in the completed (old) walls of growing cells, less than 0.5% of the peptidoglycan retains the terminal D-alanine (13, 22). Cross-links occur between two peptides by transpeptidation between the D-alanyl-D-alanine terminal peptide link of the donor pentapeptide and the free amino group of the diaminopimelic acid (DAP) of a nearby peptide (usually a tetrapeptide). However, 35% of the peptides are uncross-linked. Cross-links also occur as trimers or as DAP-DAP bonds (22).

In the tetrapeptide, the ionizable groups are the alpha-carboxyl group of the glutamic acid (pK = 4.6), the carboxyl group of the terminal alanine (pK = 4.5), the epsilon carboxyl group of DAP (pK = 3.75), and the epsilon amino group of DAP (pK = 10.2) (for a review, see reference 41). Consequently, the net charge of the tetrapeptide ranges from −3 to 1. In the basic cross-linked peptidoglycan structure containing eight amino acids, the average of the charges of all ionizable groups ranges from −2.5 to 0.5 per muramic acid molecule. To calculate the charge range of the preparations of sacculi, additional factors must be included: (i) other minor types of cross-linkings, (ii) deacetylated amino sugars (amino pK = 5.7) (5% from our chemical determinations), and (iii) lysine residues (amino pK = 10.2) left after trypsin hydrolysis of the lipoprotein. Since there is one lipoprotein molecule per nine disaccharides (3, 5), there is one lysine epsilon amino group remaining attached for every nine DAP molecules after trypsin hydrolysis. These factors give a

* Corresponding author.

charge range to −2.6 to 1.1 per muramic acid molecule, consistent with our findings.

There is a range of estimates of the sacculus thickness of *E. coli* in the literature. They vary from a single stretched monolayer to three unstretched monolayers (3, 27, 38, 39). Even if the larger amount is correct, there is no reason to doubt the hypothesis that there is only one stress-bearing layer. The most recent measurement was made with low-angle neutron scattering of sacculus preparations (52). This technique gives more information than previous methods, and a best-fitting model was proposed (52) in which 75 to 80% of the *E. coli* sacculus area is monolayer and 20 to 25% is triple layered. These literature values will be discussed below in relation to our experimental results.

In the present study, low-angle laser light scattering was used to nondestructively measure the mean sacculus surface area. This method was chosen since the measurements are not affected by the fixation and drying artifacts common with electron microscopy. It was found that the sacculi of *E. coli* could be expanded and contracted reversibly over a fourfold range in area. The mean sacculus surface area in low-ionic-strength media at a neutral pH was comparable to the mean surface area of intact cells grown under the same conditions used by Nanninga and Woldringh (58, 75). In comparison, other work from our laboratory (31, 47) showed that *E. coli* cells shrank 45% in surface area when the turgor pressure was eliminated by detergent treatment. It was concluded that a growing cell's sacculus is stretched only slightly compared with the degree that the isolated sacculus can be stretched in vitro.

Theory for the calculation of mean surface area of sacculi. The theory and computer programs for calculating surface areas of ellipsoidal shells of revolution (8, 24–26, 29, 30, 33, 35, 43, 57, 76) are briefly summarized in this section. Bacteria have dimensions comparable to the wavelengths of visible light. The light scattered from particles much smaller than the examining wavelength of light does not depend on size and shape. But even in that case, 10 parameters to calculate the absolute intensity of the light scattered in a given direction are needed. The Rayleigh formula for the case of very small particles is

$$I = \frac{8\pi^2 r^6 n_0^4}{R^2\lambda^4}\,\frac{[(n/n_0)^2 - 1]^2}{[(n/n_0)^2 + 2]^2}\,\nu I_0 \nu[1 + \cos^2(\theta)]$$

In this equation, I is the intensity of the scattered light, r is the radius of the spherical equivalent of the actual particle, n_0 is the index of refraction of the suspending medium, n is the index of refraction of the particle, ν is the particle concentration, I_0 is the intensity of the incident light, ν is the illuminated volume, θ is the angle of observation, R is the distance of the observer from the sample, and λ is the wavelength of light in vacuo. The only quantity depending on the angle of observation is shown by one of the two terms within brackets, i.e., $[1 + \cos^2(\theta)]$. These two terms account for the two perpendicular components of polarized light that compose nonpolarized light.

If a particle's radius is comparable to the wavelength of light in the suspending medium (i.e., where $\lambda' = \lambda/n_0$), then the shape, size, and orientation become very important. This, as mentioned above, is the case for many kinds of bacteria and for their isolated sacculi. If the particle's mass is too small to cause significant phase shifts of the light passing through it, then the above equation applies when amended by multiplication with an appropriate P function. There are available P functions for a variety of shapes, sizes, and orientations of particles. For ellipsoidal shells of revolution, the P function (40) depends on λ', $\theta/2$, β (the angle of orientation of the ellipsoid's major axis), a (the semiminor axis), A (the axial ratio), and B (the ratio of the semiminor axis on the inside of the shell relative to that on the outside). This last factor is a measure of the thickness of the sacculus wall.

In spite of the large number of variables, light scattering is useful for size and shape determination by comparing light scattered in different directions from the same suspension of particles. In the expressions for the ratio of light scattered in different directions, almost all of the parameters in the Rayleigh formula cancel out. Our computer program (35) calculates the relative angular light-scattering intensities of a randomly oriented suspension of ellipsoidal shells of revolution over a twofold size distribution, the same range expected for the walls prepared from cells in exponential growth. The program requires the value of the axial ratio of the sacculi or newly divided cell sacculi, A, and the factor describing the thickness of the sacculi, B. The computer program then makes the best match (least squares fit) of the observed light-scattering data and the calculated light-scattering intensities to get the best measure of the of a single parameter, a, the width of the ellipsoid of revolution. The program then computes the area and the volume of the mean ellipsoidal shell of revolution.

MATERIALS AND METHODS

Bacterial strains and culture conditions. *E. coli* B/r H266 was obtained from Conrad Woldringh. The doubling time of cultures in 1% (wt/vol) brain heart infusion broth (BHIB) was 23 min at 37°C, and in L-alanine minimal medium (77), it was 144 min at 37°C; these can be compared with published doubling times for the same strain of 22 and 136 min in the two media (77).

Media. Minimal L-alanine medium contained 2.0 g of NH_4Cl, 6.0 g of Na_2HPO_4, 0.25 g of $MgSO_4$, and 0.04 g of L-alanine per liter. BHIB (76) contained 10 g of BHIB (Difco) per liter. Fifteen grams of Difco agar per liter was added to make solid medium.

Preparation of sacculi and their derivatization. Because of the possibility that autolysis may occur during the time necessary to inactivate autolysins as the cells are treated with SDS and heat, we developed a method equivalent to flash pasteurization. We felt that this was necessary because, as the cell becomes hotter, the rate of enzymatic hydrolysis increases rapidly and would only to be halted when the enzymes become inactivated (74). We developed an apparatus so that log phase cultures while actively growing are pumped into one arm of a T, the other arm of which brings in 20% SDS (Calbiochem, San Diego, Calif.; electrophoresis grade, heavy metal free) at a slower rate. The Tee led to a copper coil immersed in a water bath at 95°C. In this way, there was only a small fraction of second between the time that the cells were in an aerated 37°C state and the time when they were in a 2% SDS-95°C state. The lysate was concentrated at 110 kG for 30 min, washed with high-quality distilled water, treated overnight at pH 6.7 with a mixture of 50 μg of bovine RNase per ml and 50 μg of DNase per ml at 37°C, then treated twice with 100 μg of trypsin per ml (all enzymes from Sigma Chemical Co., St. Louis, Mo.), washed six times with distilled water, and stored at 5°C.

The amino groups of the sacculi were altered with either acetic or succinic anhydride 5% (vol/vol). They were treated

for 10 min at room temperature and washed two times. In effect, acetylation, by converting an amine group to an *N*-acetyl group, prevents the nitrogen from becoming positively charged, and succinylation, on the other hand, removes the amino function and replaces it with the ionizable carboxy group (10, 20).

Sacculus concentration. Sacculus samples of unknown concentrations were suspended with a known concentration of polystyrene beads (Interfacial Dynamics Corporation, Portland, Ore.; 1.011-μm, average diameter). The stock bead concentration was measured by counting 1,000-fold diluted bead samples in a counting chamber (Hawksley, London, England). For each sample, 1,000 beads were counted. A mixture of equal volumes (25 μl) of the undiluted bead suspension (1.37×10^{11} beads per ml) and the sacculus suspension of unknown concentration were vortexed and diluted, and 0.5-μl samples were dried on copper transmission electron microscope grids (Ted Pella, Santa Ana, Calif.; tabbed pinpointer, 7HGC-400) for counting with a transmission electron microscope (302; Philips Co., Einthoven, Holland). The concentration of sacculi in the undiluted sample was calculated by using the ratio of sacculi to beads counted in the diluted samples and the initial concentration of beads.

Paper electrophoresis. The purity of acid-hydrolyzed sacculus samples was measured by high-voltage paper electrophoresis. Sacculus samples (containing 0.4 to 0.5 nmol of muramic acid) were hydrolyzed at 110°C in 6 N HCl for 24 h and then dried over KOH. The dried samples were dansylated (15) at 37°C for 1 h, and then 5-μl aliquots were spotted on Whatman 3MM filter paper presoaked in electrophoresis running buffer (19). The samples were electrophoresed at 15 V/cm for 8 h; the paper was removed from the electrophoresis apparatus, dried in a laminar flow hood, and then placed for 1 h in a glass chamber saturated with NH_4OH fumes. The paper was removed, and fluorescent amino acid and hexosamine derivatives were detected under near ultraviolet light.

Assays for muramic acid and hexosamine. Hadzija's assay (17) was used for muramic acid, with pure muramic acid as the standard (Sigma; reagent grade); the total hexosamine assay was that described by Ghuysen et al. (11). Hexosamine *N*-acetyl groups were estimated by Ludowieg's method (55).

Titrations. All titrations were done with a syringe micrometer burette by using either 6 N HCl or 6 N KOH with samples which contained 5 to 6 μmol of muramic acid. Titrations from pH 1.5 to 12.5 were calibrated with 0.1 M HCl (pH, 1.117 at 25°C), 0.046 M Na_2HPO_4 and 0.027 M Na_2HPO_4 (pH, 7.00 at 25°C), and saturated $Ca(OH)_2$ (pH, 12.56; Sigma; reagent grade). Titrations were measured with radiometer model PHM85 pH meter in a total sample volume of 3 ml. For each sample titrated, a blank without sacculi was also titrated under the same conditions.

Net sacculus charge measurement. The average net charge per muramic acid molecule was calculated as follows. Total acidic groups in the sacculus sample were estimated by the amount of acid required to bring the sample from pH 7 to 1.5 in 1 M KCl–50% (vol/vol) acetone. Total basic groups were estimated from the amount of base required to bring the sample from pH 7 to 12.5 in 1 M KCl–1.85% (vol/vol) formaldehyde. Acetone raises the pKs of acidic (carboxyl) groups, and formaldehyde lowers the pKs of basic (amino) groups, so the quantity of acidic and basic groups could be estimated (after correction for the blank titration).

In the light-scattering studies, it was necessary to use small samples (30 nmol of muramic acid). This amount is too small to prepare accurate titration curves. From the pHs observed during these experiments, the net charge per muramic acid molecule could be calculated from the titration curves prepared from samples which had 5 to 6 μmol of muramic acid.

Low-angle laser light-scattering apparatus assembly. A 5-mW helium-neon laser (Spectra-Physics, La Jolla, Calif.) which emitted red unpolarized light at a wavelength of 632.8 nm was used for all light-scattering experiments. The laser was placed in a cradle attached to a large board to which a large turntable was also attached. Sample suspensions of 10^9 sacculi per ml were placed in a quartz sample cuvette (2 by 2 cm), which was positioned on a small, nonrotating metal platform centered on the turnable. A small metal cradle attached to the turntable held an assembly of nested brass tubes. Light passed through only the central 30-cm-long tube, which had an inside diameter of 0.97 mm and ended in a silicon detector (PIN-5DP; United Detector Technologies, Culver City, Calif.), with its light-sensitive surface area reduced to 0.739 mm^2. The cuvette face was 25 cm from the light-collecting opening of the tube. The silicon detector signals were amplified 10^8 to 10^{10}-fold by an amplifier (101 C; United Detector). The voltages were measured by a liquid crystal display voltmeter (3468 B Multimeter; Hewlett-Packard, Palo Alto, Calif.) and printed on a thermal printer (HP-IL 8216 9-A; Hewlett-Packard). The scattering angles were measured in 2° increments from 4 to 12° from the laser beam's direction of travel. An average of six readings at each angle were taken; if a reading was very different from the other five, it was discarded and the remainder was averaged. Because light is refracted on exiting the cuvette, Snell's law was used to calculate the actual angle of light scattered within the cuvette.

To align the apparatus, the beam turntable was set at 0°C. The photodetector was removed, and the laser was adjusted so that the beam just filled the diameter of the tube and cast a circular spot without diffraction or interference patterns on a card held behind the tube. The cuvette's face was aligned perpendicularly to the laser beam so that the reflected portion retraced its path into the laser.

RESULTS

Chemical analysis of the sacculi. Acid-hydrolyzed samples of sacculi from BHIB-grown cells analyzed by paper electrophoresis had the expected peptidoglycan components: hexosamine (muramic acid and glucosamine could not be resolved), alanine, *meso*-DAP, and glutamic acid. The lysine/muramic acid molar ratio was about 1:10. Lysine is the amino acid attaching *meso*-DAP to the rest of the Braun lipoprotein (3–5). There was less than 0.01 mol of arginine per muramic acid molecule; and since arginine is 6.01% of *E. coli* cell protein (63), it follows that no more than three nonpeptidoglycan amino acids are present per 100 muramic acid molecules.

Fraction of the light-scattering signal due to nonpeptidoglycan components. *E. coli* sacculi can contain glycogen granules (54, 65), and 8.4% of the 6,000 sacculi from cells grown on BHIB observed in the electron microscope in this study were found to contain at least one lozenge-shaped particle. The contribution of the light scattered from 4 to 12° by nonpeptidoglycan impurities was estimated by measurements of light scattering after exhaustive lysozyme treatment (20 μg/ml) for 36 h at pH 6.8. Only 6.18% of the light scattered at 4° and 2.75% of the light scattered at 12° were due to lysozyme-insensitive components. When the light-

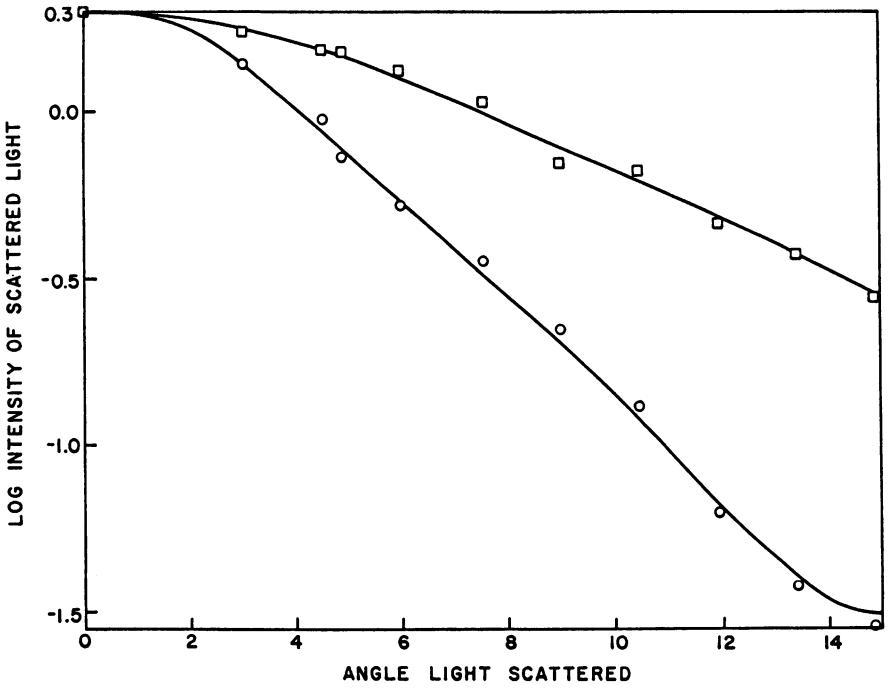

FIG. 1. Light-scattering intensity versus scattering angle for BHIB- and L-alanine-grown sacculi. Symbols: □, experimental scattering intensities for L-alanine sacculi; ○, experimental scattering intensities for BHIB sacculi. The solid lines are the best fits calculated from the light-scattering intensities under the assumption that the sacculi are a population of ellipsoidal shells of revolution. Measurements were made at 2, 4, 5, 6, 8, 12, and 14°. The angles at which the light was scattered after passage from the cuvette were corrected with Snell's law to give the angles at which the light was scattered while still in the cuvette. Scattering intensities at the corrected angles were compared with theoretical light-scattering intensities for the same angles. In the fitting process, it was assumed that the axial ratio of the cells at birth (A) was 2.45 and that the wall thickness was 0.005 of the radius, fixing B at 0.995. Both the calculated and experimental light-scattering values were normalized so that the scattered intensity at 0° was 2. The best-fitting, computer-calculated radius and area were 0.47 μm and 11.25 μm^2, respectively, for BHIB-grown sacculi and 0.29 μm and 3.79 μm^2, respectively, for L-alanine-grown sacculi.

scattering data were corrected for nonpeptidoglycan light scattering, the computer-calculated mean sacculus surface area was decreased by 8.1%. This correction was not applied to the data presented below.

Effect of aggregation. Aggregation of sacculi would decrease the scattered-light intensity at higher angles, causing overestimation of the mean surface area. The sacculus aggregation was discounted for the measurements reported here for several reasons. Most importantly, deliberately made aggregates just sufficient to affect the scattering of light contained at least a dozen sacculi and could be seen by phase-contrast microscopy; however, in samples used for light scattering, no aggregates were observed either by phase or electron microscopy.

Examination by electron microscopy. Of 6,000 sacculi from BHIB grown cells, 9.82% of the sacculi had minor damage. Evidence for normal growth was that 32.8% of the sacculi showed construction. Trueba and Woldringh (69) reported that 27.8% of cells had constrictions under the growth conditions that we had emulated in preparing our cell samples.

Electron-dispersive X-ray analysis. Sacculi contained approximately one gold and one copper atom per 10 muramic acid molecules; these metals were probably electron microscope contaminants. Magnesium, calcium, and iron were undetectable in 2 mg of sacculi.

Testing of the light-scattering technique. The ratio of the light-scattering intensities at 5 and 20° (I_5/I_{20}) is a sensitive test for the effects of multiple scattering (25, 26, 70) and was constant from 8.76×10^8 to 1.2×10^{10} sacculi per ml. At higher concentrations of sacculi, the ratio decreased, suggesting multiple scattering. At lower concentrations of sacculi, the ratios fluctuated from one sample to the next because sample scattering intensities were nearly equal to that of the distilled water blanks. The experiments reported below were done with the concentration fixed at 10^9 sacculi per ml.

Angular light-scattering data and measurement of sacculus area. The computer program (35) is based on the assumption that the sacculi approximate prolate ellipsoids of revolution. The observed angular dependence for light scattered by BHIB and L-alanine sacculi is shown in Fig. 1; the best-fitting, computer-generated scattering curves are also shown. The fitting program normalizes the curve so that it has a value of 2 (i.e., the value of $[1 + \cos^2(\theta)]$, applicable for unpolarized light at 0°), by fitting a single-scale parameter C (C contains all of the constant factors of the Rayleigh formula, given above, and some of those contained within the P function [35]). It can be seen that the light-scattering data match the fitted curves for average sacculus radii of 0.47 and 0.29 μm in the BHIB and L-alanine media, respectively, on the basis of assumptions that the axial ratio of newly divided cells in either medium (A) is 2.45 and that the ratio of the inner to the outer diameter of the sacculus (B) is 0.995.

The size of the gram-negative enteric organisms *E. coli* and *Salmonella typhimurium* (43, 59, 75) depends on their growth rate. The doubling times reported by Woldringh and Nanninga at the University of Amsterdam, (75), were 20 min

TABLE 1. Mean sacculus surface area of BHIB-grown cells after various treatments[a]

Cell component and treatment	Mean surface area (μm^2)
Sacculi[b]	
pH 4.8, 1 M KCl	6.1
pH 1.5, H_2O	22.5
pH 1.5, urea	24.5
pH 12.5, urea	20.4
pH 6.0, acetylated	21.5
pH 6.0, succinylated	25.9
Whole cells[c]	
Agar filtered, OsO_4	6.9
Agar filtered, glutaraldehyde	8.1
Phase contrast	8.6

[a] Values were derived from measurements from this study (sacculi) and estimates of Woldringh (whole cells) (75). All values refer to experiments with strain B/r H266 grown in BHIB at 37°C with aeration.

[b] Growing cells were harvested, lysed with SDS, purified with trypsin, washed extensively, and analyzed by the low-angle light-scattering method developed here.

[c] Data from C. Woldringh for agar-filtered cells fixed with either osmium tetroxide or glutaraldehyde and for living cells as determined by phase-contrast microscopy.

for BHIB-grown cells and 135 min for L-alanine minimal medium-grown cells, compared with our data of 24 and 146 min, respectively, for identical conditions. Assuming that the cells were cylinders with hemispherical poles, the calculated surface areas would be 11.25 and 3.79 μm^2, respectively, with a ratio of 2.97. The best computer-fitted curve to the light-scattering data (Fig. 1) gave values of 7.9 and 3.1 μm^2, respectively, with a ratio of 2.5.

Wall dimensions and composition. The analytical result observed here is that there are 10^6 chemically determined muramic acid molecules per BHIB sacculus counted by electron microscopy. The mean sacculus surface area under the most compact conditions (pH 4.8, 1 M KCl) is 6.1 μm^2 (Table 1). This is not too different from the area for the average cell grown in rich medium (7.1 μm^2) (42, 58, 73). Consequently, there is one muramic acid molecule per 0.68 nm^2 of saccular surface at pH 7.0. This result conflicts with recent results (73) of 2.5 μm^2 per DAP molecule. It is not certain which of several possibilities accounts for the discrepancy. Assuming our value of 1×10^6 muramic acid residues per sacculus, it is possible to cause the charge to range from 10×10^6 positive charges to 28×10^6 negatively charged groups per average sacculus.

The smallest minimally stressed sacculus is 3.48 μm long and 1.26 μm wide at the isoelectric point of peptidoglycan (58). This accords with the mean sacculus surface area of 6.1 μm^2 reported in Table 1 for the sacculi from cultures grown in BHIB.

Mean surface area as a function of charge, ionic strength, pH, and acylation of the sacculi. The mean sacculus surface areas of BHIB-grown cells tested under various conditions are presented in Table 1. They are expressed as the average area of the sacculus. The smallest mean surface area was observed under isoionic pH conditions at high ionic strength. Under these conditions, the sacculi are still ellipsoids of revolution as determined by comparison to the electron microscopic observations. The succinylation of sacculus amino groups eliminates them and adds carboxyl groups, yielding a charge of −2.6 per muramic acid molecule at pH 7.0. On the basis of the pKs of the titratable groups, it was assumed that there were no positive charges at pH 12.5 and no negative charges at pH 1.5. At pH extremes and after succinylation, the mean sacculus surface area ranged from 20 to 26 μm^2, which is 200 to 300% greater than the isoionic (minimum) area. The important generalization is that roughly the same expansion of the peptidoglycan fabric can be obtained in a number of different ways, suggesting that the maximum expansion of the fabric without breaking covalent bonds is 20 to 26 μm^2.

Titration reversibility. Figure 2 shows the net charge and mean sacculus surface area from pH 1.5 to 12.5. The experiments were actually carried out by titrating from a neutral pH to each extreme of pH and back. These data are not shown, but the forward and reverse titrations were nearly superimposable (36, 74). This suggests that there is little hysteresis in either sacculus expansion and contraction or in the accessibility of titratable peptidoglycan groups to the medium. It should be noted that the expansion is highly cooperative (19, 66), and only when a sufficient net charge is developed are there major conformational changes. It should also be noted that the net charge calculated from the pKs and amounts of different titratable groups in the wall preparation is 0 at a pH slightly below 4. This is consistent with the isoelectric point of peptidoglycan preparations and implies that placing a positive charge on the sacculi with acid causes dramatic expansion, whereas the first two negative charges formed as the pH is increased are not effective in expanding the wall and the third one causes an expansion, although not quite as extreme as that caused by acid. The implication is that the isolated carboxyl group on the glutamic acid residues, the free carboxyl groups of D-alanine, and the epsilon carboxyl of DAP, whose adjacent amino group is engaged in peptide bond formation, have little effect on the size of the sacculus. On the other hand, the free zwitterions of DAP are crucial, and the conversion at a low pH to an isolated, positively charged group or its conversion via succinylation to a negatively charged group at high pH is enough to cause expansion.

DISCUSSION

Peptidoglycan is formed into a strong, but elastic fabric which resists the expansive effects of the cell's turgor pressure. The elasticity of this network is the cornerstone of the surface stress theory, particularly as applied to gram-negative microorganisms (28, 32). The theory postulates that nascent oligopeptidoglycan strands in their relaxed conformation become linked at multiple points to existing strands. The nascent strands are subsequently stretched into an extended conformation when cleavages of an old stress-bearing wall occurs, thereby stressing the new wall and permitting growth and enlargement of the sacculus and an increase in the cell volume. Thus, a cycle operates with the following seven stages: (i) biosynthesis of the cytoplasm, (ii) increase in turgor pressure, (iii) increase in stress in the wall, (iv) increase in the autolytic action upon the existing wall, (v) transfer of stress to the new wall, (vi) stretching of the nascent oligopeptidoglycan strands, and (vii) increase in the area of the sacculus, increasing the cellular volume and lowering the turgor pressure. The present work (Table 1 and Fig. 2) demonstrates the great elasticity of the gram-negative sacculus. Marquis and coworkers (56, 61, 62) observed that fragments of the thick, gram-positive bacterial walls expanded at pH extremes. Their quantitative observations of volume changes are consistent with the wall surface area changes reported here. Thwaites and Mendelson (67) found

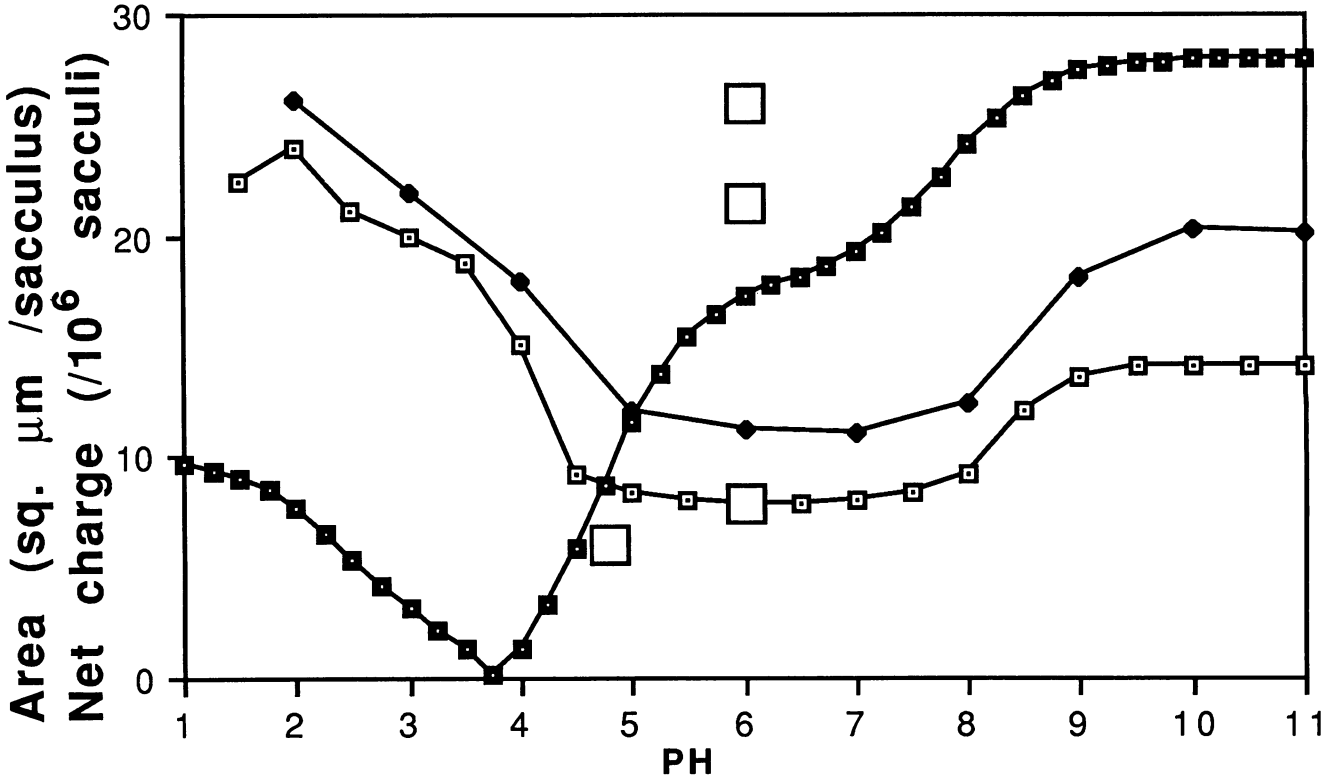

FIG. 2. Mean sacculus surface area as a function of pH. As the experimental data were recorded, acidic titrations started at pH 6.0 and ended at pH 1.5 and the samples were titrated in reverse; similarly, basic titrations started at pH 6.0 and ended at pH 12.5 and were then reverse titrated. The light-scattering measurements under different conditions were converted into areas of ellipsoidal shells of revolution and are reported as square micrometers. The mean sacculus surface area as a function of pH in the absence (⊡) and presence (◆) of 10.1 M urea is shown. Succinylated sacculi, acetylated sacculi, untreated sacculi at the same pH, and untreated sacculi in 1 M KCl are shown from top to bottom, respectively (□). The theoretical net charge (■) is the average charge per 10^6 sacculi calculated from the composition of the sacculi given in the text and the pK values of the ionizable groups.

that cablelike threads composed of *B. subtilis* filaments have viscoelastic mechanical properties, but their studies do not distinguish between the peptidoglycan properties of individual cells and those related to the interactions of different cellular filaments within the thread.

Although there have been no studies of the elastic properties of the sacculi of gram-negative bacteria, there have been many studies of volume changes of osmotically stressed, gram-negative bacteria (for reviews, see references 9 and 31). While these size changes have been usually interpreted in terms of plasmolysis only, shrinkage of the taut cell fabric is important for gram-negative bacteria. We were able to show that a growing *E. coli* filamentous mutant decreased 17% in length when the cytoplasmic membrane was ruptured with a detergent that eliminated the cell turgor pressure (47). This corresponds to the mean sacculus surface area of the growing cell being 45% greater than the relaxed conformation.

A possible interpretation of this contraction caused by rupturing the lipid membranes is that the wall of the growing cell is stretched to its elastic limit during growth and shrinks to its relaxed conformation when the hydrostatic stress is removed. This is far from correct since the results reported here prove that isolated sacculi can reversibly increase in area much more than 45%, to at least 300% above the relaxed conformation. The disparity in our earlier in vivo results with growing cells (47) and the current in vitro studies of intact sacculi probably means either that the comparison with the electron microscope studies is invalid and the wall is in a partially extended configuration due to interactions with the inner and outer membranes even after disruption with detergent or, more likely, that the sacculus under growing conditions is never stretched enough to approach its elastic limit. This finding will obviously be very important in the further elucidation of the mechanics of bacterial growth.

While our results do not prove that stronger stresses could not result in further expansion, the sacculus reversible expansion of 300% above the released conformation area reported here is consistent with molecular models of peptidoglycan (4, 5, 7, 44, 50, 51, 60). While the glycan chains are quite inextensible, the peptides can have conformations varying from a compact to an extended conformation sufficient to account for a fourfold length difference and hence a 300% increase in area upon extension as well.

Fundamental unit of cell wall fabric. The area of the cell protected by a structural unit of wall, not just the linear course in the polymer of either the cross-linked peptides or glycan chains, is the subject at hand. The unit of the two-dimensional network is a ring with glycan and peptide elements, each of which is part of other rings. For example, the entity that is a hexagon of wire in the familiar case of chicken wire is the fundamental unit of that fabric. As in that case, a segment of wire (or in the bacterial case, a portion of glycan chain or cross-linked peptide) defines the limits of the

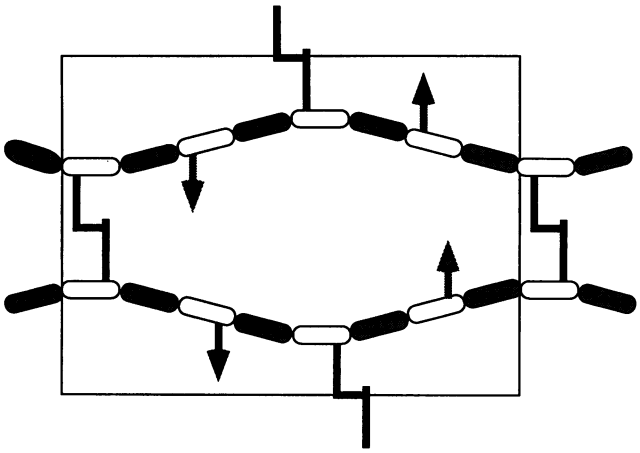

FIG. 3. Structure of a stressed unit of the wall fabric. Inside of the boxed area are two oligopeptidoglycan chains connected by cross-links in two places to each other. The model is based on the supposition that it takes four disaccharides to allow the glycan chain to go through a complete rotation. In the unit outlined by the box, two peptides are not part of the unit but extend outward in the plane to be part of the adjacent units. In addition, a pair of peptides point upward and may connect to more peripheral wall. The other pair faces inward and forms bonds to a more-central murein. Neither pair would be part of the fundamental ring unit. The structure as depicted is for the conformation of ring units of isolated sacculi at pH extremes or in the chemically modified sacculi. In an intact, growing cell, there is a much-less-expanded structure (expanded over the most compact state by 45%). If the cell membrane is ruptured, then the unit contracts further as the covalent bonds adjust to their lowest energy, subject still to the constraint that the wall is a covalent fabric; this relaxed isoionic form would have about one-fourth of the area of the unit shown here.

individual unit. The smallest possible unit of cross-linked, two-dimensional peptidoglycan is diagrammed in Fig. 3. A smaller one was suggested previously (45), but it is not possible because the hexosamines of the glycan chains of the murein rotate relative to each other in such a way that a complete revolution requires about four disaccharides (1, 2, 7, 49, 50, 51, 53). This means that the region enclosed in the rectangle (Fig. 3) is the unit of peptidoglycan such that many of them when overlaid could totally cover the surface of a bacterium. The structure shown is two decasaccharides connected by two pairs of cross-linked peptides emanating from the first and ninth saccharides of both chains. The cross bridges are formed by the usual head-to-tail linkage of D-alanine of one strand with the epsilon amino group of DAP on the other. The third and seventh saccharides of both chains would be muramyl glycosides, with their lactyl groups pointing above or below the plane of the figure. Obviously, other rings with different connections between the parts also occur in the stress-bearing wall. The peptides originally linked at the third and seventh positions may be quickly cleaved, serve in linking nascent oligopeptidoglycan, or serve in links to oligopeptidoglycan that has yet to be discarded. In any case, these peptides are not serving the function of covering the cell surface area in a stress-bearing way.

Implications of the in vivo structure not being maximally extended. The results reported here are quite unexpected in two ways. The finding that the relaxed sacculus can readily expand 300% in area with quite minimal stress seems contradictory to the finding that the wall in vivo is expanded only 45% above the turgor-free state. There are two interpretations of these results. The first, a less-likely explanation, is that the inner and outer membranes truly contribute a good deal to supporting the stress due to turgor and keep the wall from expanding to its fullest extent; it is not clear how they could do this, and this interpretation would appear to contradict the electron microscope studies cited above. The second explanation is that turgor pressure does not create as strong a tension in the wall as the electrostatic repulsion that we applied by causing the sacculi to bear a net positive or negative charge.

The second unexpected result of this study is the key role of the epsilon group of DAP not engaged in peptide bond formation. When the carboxyl and amino groups are adjacent to each other, they cause the pK of each to be more extreme. The finding that expansion is associated with destruction of the zwitterion shows that this part of the sacculus is the key to its expansion. Actually, unlinked DAP residues are an appendage to the stress-bearing peptide, but being changed from the zwitterion to a single charge of either sign seems to be crucial. This finding may be particularly important in considering the implications of different elasticities of the peptidoglycan in influencing the shapes of the poles of *Bacillus subtilis* and *Enterococcus hirae* (41).

Implications for the growth of gram-negative organisms. Because most of the peptidoglycan of *E. coli* is a monolayer (53), the gram-positive model of inside-to-outside elongation of the side wall (45, 48), as suggested by Glauner et al. (13), cannot apply. The neutron-scattering data would be consistent only with an insertion, linkage, and cleavage of old bonds, with the tensile forces pulling the new peptidoglycan into the stress-bearing surface. This implies the existence of some very special, precisely regulated mechanism to cleave the old wall (39). It is no doubt the case that nonstress-bearing nascent material added but not yet pulled into the surface and nonstress-bearing wall in the process of being turned over contribute to the portion of the wall that appears to be triply layered. Also, the deep constrictions associated with the initial phases of cell division could contribute to the multiply layered region. If the inside-to-outside model functioned for gram-negative organisms, then several complete layers, in addition to layers of wall in the act of being inserted or being discarded, would be expected. The present work also suggests that there is only a single layer of fabric; if parts of the wall had different numbers of layers, one could expect the expansion to have occurred in stages instead of one cooperative process.

It should be noted that the neutron data and the results presented here are consistent with the "patches" model of Höltje and Glauner (21) if the patches are both small and numerous and if one or the other of my suggestions (39) of an allosteric enzyme or a holoenzyme direct a make-before-break process. In any case, the patch must be so small that its insertion into the fabric does not depend on stresses of different magnitudes in the hoop and axial directions. Then the cleavage of old wall would pull the new wall into the stress-bearing layer and would lead to elongation without catastrophic dilation of the cell.

ACKNOWLEDGMENTS

We thank Paul Demchick, Suzanne Pinette, and David White for help.

We acknowledge an equipment grant from Allan Audio, Bloomington, Ind.

REFERENCES

1. **Barnickel, G., H. Labischinski, H. Bradaczek, and P. Giesbrecht.** 1979. Conformational energy calculation on the peptide part of murein. Eur. J. Biochem. **95:**157–165.
2. **Barnickel, G., D. Naumann, and H. Bradaczek.** 1983. Computer-aided molecular modelling of the three-dimensional structure of bacterial peptidoglycan, p. 61–66. *In* R. Hakenbeck, J.-V. Höltje, and H. Labischinski (ed.), Target of penicillin. Walter de Gruyter & Co., New York.
3. **Braun, V.** 1975. Covalent lipoprotein from the outer membrane of *Escherichia coli*. Biochim. Biophys. Acta **415:**335–377.
4. **Braun, V., H. Gnirke, U. Henning, and K. Rehn.** 1973. Model for the structure of the shape-maintaining layer of the *Escherichia coli* cell envelope. J. Bacteriol. **114:**1264–1270.
5. **Braun, V., and U. Sieglin.** 1970. The covalent murine-lipoprotein structure of the *Escherichia coli* cell wall. The attachment site of the lipoprotein on the murein. Eur. J. Biochem. **13:**336–346.
6. **Burge, R. E., R. Adams, H. H. M. Balyuzi, and D. A. Reaveley.** 1977. Structure of the peptidoglycan of bacterial cell walls. II. J. Mol. Biol. **117:**955–974.
7. **Burge, R. E., A. G. Fowler, and D. A. Reaveley.** 1977. Structure of the peptidoglycan of bacterial cell walls. I. J. Mol. Biol. **117:**927–953.
8. **Cross, D. A., and P. Latimer.** 1972. Angular dependence of scattering from *Escherichia coli* cells. Appl. Opt. **11:**1225–1228.
9. **Csonka, L. N.** 1989. Physiological and genetic response of bacteria to osmotic stress. Microbiol. Rev. **53:**121–147.
10. **Doyle, R. J., T. H. Matthews, and U. N. Streips.** 1980. Chemical basis for selectivity of metal ions by *Bacillus subtilis* cell wall. J. Bacteriol. **143:**471–480.
11. **Ghuysen, J.-M., D. J. Tipper, and J. L. Strominger.** 1966. Enzymes that degrade bacterial cell walls. Methods Enzymol. **10:**685–700.
12. **Glauner, B., and J.-V. Höltje.** 1990. Growth pattern of the murein sacculus of *Escherichia coli*. J. Biol. Chem. **265:**18988–18996.
13. **Glauner, B., J.-V. Höltje, and U. Schwarz.** 1988. The composition of the murein of *Escherichia coli*. J. Biol. Chem. **263:**10088–10095.
14. **Glauner, B., and U. Schwarz.** 1983. The analysis of murein composition with high-pressure-liquid chromatography, p. 29–34. *In* R. Hakenbeck, J.-V. Höltje, and H. Labischinski (ed.), Target of penicillin. Walter de Gruyter & Co., New York.
15. **Gray, W. R.** 1968. Dansyl chloride procedure. Methods Enzymol. **12:**139–151.
16. **Gross, D.** 1961. An apparatus for high-voltage paper electrophoresis. J. Chromatogr. **5:**194–206.
17. **Hadzija, O.** 1974. A simple method for the quantitative determination of muramic acid. Anal. Biochem. **60:**512–517.
18. **Harz, H., K. Burgdorf, and J.-V. Höltje.** 1990. Isolation and separation of the glycan strands from murein of *Escherichia coli* by reversed-phase high-performance liquid chromatography. Anal. Biochem. **190:**120–128.
19. **Hiemenz, P. C.** 1986. Principles of colloid and surface chemistry, 2nd ed. Marcel Dekker, Inc., New York.
20. **Hoare, D. G., and D. E. Koshland, Jr.** 1967. A method for the quantitative modification and estimation of carboxylic acid groups in proteins. J. Biol. Chem. **242:**2447–2453.
21. **Höltje, J.-V., and B. Glauner.** 1990. Structure and metabolism of the murein sacculus. Res. Microbiol. **141:**75–89.
22. **Höltje, J.-V., and U. Schwarz.** 1985. Biosynthesis and growth of the murein sacculus of *Escherichia coli*, p. 77–119. *In* N. Nanninga (ed.), Molecular cytology of *Escherichia coli*. Academic Press Ltd., London.
23. **Höltje, J.-V., and E. I. Tuomanen.** 1991. The murein hydrolases of *Escherichia coli*: properties, functions and impact on the course of infections *in vivo*. J. Gen. Microbiol. **137:**441–454.
24. **Jovin, T. M., S. J. Morris, G. Striker, H. A. Schultens, M. Digweed, and D. J. Arndt-Jovin.** 1976. Automatic sizing and separation of particles by ratios of light scattering intensities. J. Histochem. Cytochem. **24:**269–283.
25. **Koch, A. L.** 1961. Some calculations on the turbidity of mitochondria and bacteria. Biochim. Biophys. Acta **51:**429–441.
26. **Koch, A. L.** 1968. Theory of angular dependence of light scattered by bacteria and similar-sized biological objects. J. Theor. Biol. **18:**133–156.
27. **Koch, A. L.** 1982. On the growth and form of *Escherichia coli*. J. Gen. Microbiol. **128:**2527–2540.
28. **Koch, A. L.** 1983. The surface stress theory of microbial morphogenesis. Adv. Microbial Physiol. **24:**301–366.
29. **Koch, A. L.** 1983. The shapes of Gram-negative organisms: variable T models, p. 99–104. *In* R. Hakenbeck, J. Höltje, and H. Labischinski (ed.), The target of penicillin. Walter De Gruyter & Co., Berlin.
30. **Koch, A. L.** 1984. Turbidity measurements in microbiology. ASM News **50:**473–477.
31. **Koch, A. L.** 1984. Shrinkage of growing *Escherichia coli* cells by osmotic challenge. J. Bacteriol. **159:**914–924.
32. **Koch, A. L.** 1984. How bacteria get their shapes: the surface stress theory. Comments. Mol. Cell Biophys. **2:**179–196.
33. **Koch, A. L.** 1986. Estimation of size of bacteria by low-angle light-scattering measurements: theory. J. Microbiol. Methods **5:**221–235.
34. **Koch, A. L.** 1988. Biophysics of bacterial wall viewed as a stress-bearing fabric. Microbiol. Rev. **52:**337–353.
35. **Koch, A. L.** 1989. Calculation of surface area of sacculi from low-angle light scattering measurements. J. Microbiol. Methods **9:**139–150.
36. **Koch, A. L.** 1990. The sacculus contraction/expansion model for gliding motility. J. Theor. Biol. **142:**95–112.
37. **Koch, A. L.** 1990. Growth and form of the bacterial cell wall. Am. Sci. **78:**327–341.
38. **Koch, A. L.** 1990. The surface stress theory for the case of *E. coli*: the paradoxes of gram-negative growth. Res. Microbiol. **141:**119–130.
39. **Koch, A. L.** 1990. Additional argument for the key role of "smart" autolysins in the enlargement of the wall of gram-negative bacteria. Res. Microbiol. **141:**529–541.
40. **Koch, A. L.** 1990. Recent extensions of the surface stress theory, p. 39–63. *In* R. K. Poole and M. J. Bazin (ed.), Microbial growth dynamics. Oxford University Press, Oxford.
41. **Koch, A. L.** 1991. Differences in the formation of poles of *Enterococcus* and *Bacillus*. J. Theor. Biol. **154:**205–217.
42. **Koch, A. L., and I. D. J. Burdett.** 1984. The variable T model for Gram-negative morphology. J. Gen. Microbiol. **130:**2325–2338.
43. **Koch, A. L., and E. Ehrenfeld.** 1968. The size and shape of bacteria by light scattering measurements. Biochim. Biophys. Acta **165:**262–273.
44. **Koch, A. L., and J. Gajewski.** 1991. Unpublished calculations.
45. **Koch, A. L., M. L. Higgins, and R. J. Doyle.** 1981. Surface tension-like forces determine bacterial shapes: *Streptococcus faecium*. J. Gen. Microbiol. **123:**151–161.
46. **Koch, A. L., M. L. Higgins, and R. J. Doyle.** 1982. The role of surface stress in the morphology of microbes. J. Gen. Microbiol. **128:**927–945.
47. **Koch, A. L., S. L. Lane, J. A. Miller, and D. G. Nickens.** 1987. Contraction of filaments of *Escherichia coli* after disruption of the cell membrane by detergent. J. Bacteriol. **169:**1979–1984.
48. **Koch, A. L., H. L. T. Mobley, R. J. Doyle, and U. N. Streips.** 1981. The coupling of wall growth and chromosome replication in Gram-positive rods. FEMS Microbiol. Lett. **12:**201–208.
49. **Labischinski, H., G. Barnickel, H. Bradaczek, and P. Giesbrecht.** 1979. On the secondary and tertiary structure of murein. Eur. J. Biochem. **95:**147–155.
50. **Labischinski, H., G. Barnickel, and D. Naumann.** 1983. The state of order of bacterial peptidoglycan, p. 49–54. *In* R. Hakenbeck, J.-V. Höltje, and H. Labischinski (ed.), Target of penicillin. Walter de Gruyter & Co., New York.
51. **Labischinski, H., G. Barnickel, D. Naumann, and P. Keller.** 1985. Conformational and topological aspects of the three-dimensional architecture of bacterial peptidoglycan. Ann. Inst. Pasteur/Microbiol. (Paris) **136A:**45–50.
52. **Labischinski, H., E. W. Goodell, A. Goodell, and M. Hochberg.** 1991. Direct proof of a "more-than-single-layered" peptidoglycan architecture of *Escherichia coli* W7: a neutron small-angle

scattering study. J. Bacteriol. **173:**751–756.
53. **Leps, B., G. Barnickel, H. Bradaczek, and H. Labischinski.** 1983. Comparison between the sugar chain conformation in murein and pseudomurein, p. 67–72. *In* R. Hakenbeck, J.-V. Höltje, and H. Labischinski (ed.), Target of penicillin. Walter de Gruyter & Co., New York.
54. **Leutgeb, V. W., and W. Weidel.** 1963. Uber ein in coli-zellwand-praparaten zuruckgehaltenes glykogen. Z. Naturforsch. **18b:** 1060–1062.
55. **Ludowieg, J., and A. Dorfman.** 1959. A micromethod for the colorimetric determination of N-acetyl groups in acid mucopolysaccharides. Biochim. Biophys. Acta **38:**212–218.
56. **Marquis, R. E.** 1968. Salt-induced contraction of bacterial cell walls. J. Bacteriol. **95:**775–781.
57. **Mullaney, P. F., and P. N. Dean.** 1970. The small angle light scattering of biological cells. Biophys. J. **10:**764–772.
58. **Nanninga, N., and C. L. Woldringh.** 1985. Cell growth, genome duplication, and cell division, p. 259–318. *In* N. Nanninga (ed.), Molecular cytology of *Escherichia coli*. Academic Press Ltd., London.
59. **Neidhardt, F. C., J. L. Ingraham, and M. Schaechter.** 1990. Physiology of the bacterial cell. Sinaur Associates, Sunderland, Mass.
60. **Oldmixon, E. H., S. Glauser, and M. L. Higgins.** 1974. Two proposed general configurations for bacterial cell wall peptidoglycan shown by space filling models. Biopolymers **13:**2037–2060.
61. **Ou, L.-T., and R. E. Marquis.** 1970. Electromechanical interactions in cell walls of gram-positive cocci. J. Bacteriol. **101:**92–101.
62. **Ou, L.-T., and R. E. Marquis.** 1972. Coccal cell-wall compactness and the swelling action of denaturants. Can. J. Microbiol. **18:**623–629.
63. **Rogers, H. J., H. R. Perkins, and J. B. Ward.** 1980. Structure of peptidoglycan, p. 190–214. *In* Microbial cell walls and membranes. Chapman and Hall, New York.
64. **Romeis, T., U. Kohlrausch, K. Burgdorf, and J. V. Höltje.** 1991. Murein chemistry of cell division in *Escherichia coli*. Res. Microbiol. **142:**325–332.
65. **Shively, J. M.** 1974. Inclusion bodies of procaryotes. Annu. Rev. Microbiol. **28:**167–187.
66. **Tanford, C. E.** 1960. The interpretation of hydrogen ion titration curves of proteins. Adv. Protein Chem. **15:**69–139.
67. **Thwaites, J. J., and N. H. Mendelson.** 1991. Mechanical behavior of bacterial cell walls. Adv. Microbiol Physiol. **32:**174–222.
68. **Tipper, D. J., and A. Wright.** 1979. The structure and biosynthesis of bacterial cell walls, p. 291–426. *In* J. R. Sokatch and L. N. Ornston (ed.), The Bacteria. Academic Press, Inc., New York.
69. **Trueba, F. J., and C. L. Woldringh.** 1980. Changes in cell diameter during the division cycle of *Escherichia coli*. J. Bacteriol. **142:**869–878.
70. **Van de Hulst, H. C.** 1957. Light scattering by small particles. John Wiley & Sons, Inc., New York.
71. **Ward, I. M.** 1971. Mechanical properties of solid polymers. Interscience Publishers, Inc., New York.
72. **Weidel, W., and H. Pelzer.** 1964. Bag-shaped macromolecules—a new outlook on bacterial cell walls. Adv. Enzymol. **26:**193–232.
73. **Wientjes, F. B., C. L. Woldringh, and N. Nanninga.** 1991. Amount of peptidoglycan in cell walls of gram-negative bacteria. J. Bacteriol. **173:**7684–7691.
74. **Woeste, S.** 1988. The mechanical properties of the isolated sacculus of *Escherichia coli* B/r H266. Ph.D. dissertation. Indiana University, Bloomington.
75. **Woldringh, C. L., and N. Nanninga.** 1985. Structure of the nucleoid and cytoplasm in the intact cell, p. 161–197. *In* N. Nanninga (ed.), Molecular cytology of *Escherichia coli*. Academic Press, Inc., (London) Ltd., London.
76. **Wyatt, P. J.** 1973. Differential light scattering techniques for microbiology, p. 183–263. *In* J. R. Norris and D. W. Ribbons (ed.), Methods in microbiology, vol. 8. Academic Press, Inc. (London) Ltd., London.
77. **Zaritsky, A., C. L. Woldringh, and D. Mirelman.** 1979. Constant peptidoglycan density in the sacculus of *Escherichia coli* B/r growing at different rates. FEBS Lett. **98:**29–32.